# Construction of an immunoinformatics-based multi-epitope vaccine candidate targeting Kyasanur forest disease virus

Sunitha Manjari Kasibhatla[1,*], Lekshmi Rajan[2,*], Anita Shete[2], Vinod Jani[1], Savita Yadav[2], Yash Joshi[2], Rima Sahay[2], Deepak Y. Patil[2], Sreelekshmy Mohandas[2], Triparna Majumdar[2], Uddhavesh Sonavane[1], Rajendra Joshi[1] and Pragya Yadav[2]

[1] Centre for Development of Advanced Computing, Pune, India
[2] Indian Council of Medical Research-National Institute of Virology, Pune, India
[*] These authors contributed equally to this work.

## ABSTRACT

Kyasanur forest disease (KFD) is one of the neglected tick-borne viral zoonoses. KFD virus (KFDV) was initially considered endemic to the Western Ghats region of Karnataka state in India. Over the years, there have been reports of its spread to newer areas within and outside Karnataka. The absence of an effective treatment for KFD mandates the need for further research and development of novel vaccines. The present study was designed to develop a multi-epitope vaccine candidate against KFDV using immunoinformatics approaches. A total of 74 complete KFDV genome sequences were analysed for genetic recombination followed by phylogeny. Computational prediction of B- and T-cell epitopes belonging to envelope protein was performed and epitopes were prioritised based on IFN-Gamma, IL-4, IL-10 stimulation and checked for allergenicity and toxicity. The eight short-listed epitopes (three MHC-Class 1, three MHC-Class 2 and two B-cell) were then combined using various linkers to construct the vaccine candidate. Molecular docking followed by molecular simulations revealed stable interactions of the vaccine candidate with immune receptor complex namely Toll-like receptors (TLR2-TLR6). Codon optimization followed by *in-silico* cloning of the designed multi-epitope vaccine construct into the pET30b (+) expression vector was carried out. Immunoinformatics analysis of the multi-epitope vaccine candidate in the current study has potential to significantly accelerate the initial stages of vaccine development. Experimental validation of the potential multi-epitope vaccine candidate remains crucial to confirm effectiveness and safety in real-world conditions.

**Subjects** Biochemistry, Bioinformatics, Virology, Infectious Diseases
**Keywords** Kyasanur forest disease virus, Immunoinformatics, Epitopes, Vaccine, Immune receptor

## INTRODUCTION

Kyasanur forest disease is a highly neglected emerging tick-borne viral zoonosis caused by Kyasanur forest disease virus (KFDV) that belongs to the family *Flaviviridae* (*Gould & Solomon, 2008*). The disease was first identified in 1957 in the Kyasanur forest region of Karnataka, India, and has since posed a significant public health threat, with sporadic

Submitted 5 August 2024
Accepted 22 January 2025
Published 21 March 2025

Corresponding authors
Rajendra Joshi,
rrjoshi02@yahoo.com
Pragya Yadav,
hellopragya22@gmail.com

Academic editor
Reema Singh

Additional Information and Declarations can be found on page 20

DOI **10.7717/peerj.18982**



**How to cite this article** Kasibhatla SM, Rajan L, Shete A, Jani V, Yadav S, Joshi Y, Sahay R, Patil DY, Mohandas S, Majumdar T, Sonavane U, Joshi R, Yadav P. 2025. Construction of an immunoinformatics-based multi-epitope vaccine candidate targeting Kyasanur forest disease virus. **PeerJ 13:e18982 DOI 10.7717/peerj.18982**

outbreaks occurring in newer districts of Karnataka and the states of Maharashtra, Goa, Kerala, and Tamil Nadu (*Yadav, Sahay & Mourya, 2018*; *Patil et al., 2017*; *Gladson et al., 2021*; *Tandale et al., 2015*). The mortality rate for KFDV infection is reported to be about 2–10% (*Gladson et al., 2021*; *National centre for disease control (NCDC), 2018*). Mammals and birds act as secondary hosts as well as reservoir for transmission of KFDV through ticks to the vertebrate hosts, with the main vector being the anthropophagic *Haemaphysalis spinigera* (*Boshell & Rajagopalan, 1968*; *Trapido et al., 1959*; *Work, 1958*).

KFDV is an enveloped spherical virus with single-stranded RNA of 11 kb size enclosed in the icosahedral nucleocapsid. The diameter of the virion is 40–65 nm and codes for a single polyprotein (*Dodd et al., 2011*; *Gritsun et al., 2014*). Three structural (capsid, pre-membrane (prM) and envelope) and seven non-structural proteins (NS1, NS2A, NS2B, NS3, NS4A, NS4B and NS5) are encoded by the polyprotein. The envelope (E) protein of KFDV plays an important role in the entry of the pathogen into the host cells by receptor binding and membrane fusion (*Mukhopadhyay, Kuhn & Rossmann, 2005*; *Mondotte et al., 2007*). The E protein has three domains, domain I (EDI), domain II (EDII), and domain III (EDIII). Among them, ED III is associated with the receptor binding and initiating the first step of viral entry. Although the exact cellular receptor for KFDV has not been conclusively identified, studies on closely related flaviviruses indicate that laminin receptors and dendritic cell-specific intercellular adhesion molecule 3-grabbing non-integrin (DC-SIGN) could be involved (*Piccini, Castilla & Damonte, 2015*; *Kuno, 2007*). After binding to the receptor, the virus is internalized into the host cell *via* clathrin-mediated endocytosis (*Chu & Ng, 2004*; *Van der Schaar et al., 2007*). The role of the E protein, especially EDIII, in facilitating efficient endocytosis is significant as it maintains a stable interaction with the host cell membrane during internalization. Within the endosome, the pH drops, which triggers a conformational rearrangement in the E protein. This change is crucial for viral entry as it exposes the fusion loop in EDII, which interacts with the endosomal membrane (*Modis et al., 2004*; *Zhang et al., 2003*). Once the viral and endosomal membranes fuse, the viral RNA genome is released into the host cell cytoplasm, initiating replication and protein synthesis (*Stiasny, Koessl & Heinz, 2003*; *Rothan & Kumar, 2019*). The EDIII domain is thought to revert to its original configuration post-fusion, allowing the E protein to retain functional integrity for further rounds of viral assembly and exit (*Zhang et al., 2003*). The E protein is a key immunogenic component that contains several epitopes recognized by B and T cells. It includes multiple B-cell epitopes capable of inducing neutralizing antibody responses. Additionally, the E protein plays a crucial role in T-cell activation, as vaccination strategies involving E protein constructs have been shown to enhance the activation of both CD4+ and CD8+ T cells which are essential mediators of cellular immunity. These T cells produce cytokines such as TNF-α and IFN-γ, which contribute to an amplified immune response against KFDV (*Sirmarova et al., 2018*). Furthermore, studies utilizing a vesicular stomatitis virus (VSV)-based platform expressing KFDV prM and E proteins have shown that immunized nonhuman primates develop strong neutralizing antibody titers against KFDV, as well as cross-reactive antibodies against Alkhurma hemorrhagic fever virus (AHFV), suggesting potential cross-protective benefits within the flavivirus group (*Bhatia et al., 2023*; *Bhatia*

*et al., 2021*). E-protein evokes the neutralizing antibody response, which has been demonstrated to effectively neutralize KFDV and related flaviviruses, making it a valuable target for vaccine development (*Heinz & Stiasny, 2012*).

Presently, there is no clinically approved drug against KFDV and hence affected individuals are treated based on symptoms along with supportive therapy. The formalin-inactivated KFD vaccine was one of the early measures used in preventing the disease and has been used primarily in certain regions of India where KFD is endemic. However, the primary concern with the formalin-inactivated vaccine is its hesitancy by people due to side effects at the injection site (*Dandawate et al., 1994*; *Kasabi et al., 2013b*). While it may offer some protection against KFDV, it may not provide complete or long-lasting immunity. There may be breakthrough infections among individuals who have received the vaccine. Earlier studies demonstrated the low effectiveness of the vaccine even after repeated booster doses (*Kasabi et al., 2013a*; *Kiran et al., 2015*). Besides this, the estimated mean rate of nucleotide substitution based on the complete genome of KFDV is $4.2 \times 10^{-4}$ subs/site/year (*Yadav et al., 2020*). The earliest known KFDV strain was isolated in 1957, so the virus has been in circulation since the last six decades in India. Studies have shown that KFDV can accumulate mutations in its envelope protein. Some of these mutations have been linked to changes in the antigenicity of the envelope protein, which means that the virus may become less susceptible to the immune system (*Yadav et al., 2020*; *Mehla et al., 2009*; *Shil et al., 2018*). The low efficacy of currently available vaccines and the increasing spread of KFDV to naive regions in India necessitates the need for the development of a new KFD vaccine (*Yadav, Sahay & Mourya, 2018*; *Kasabi et al., 2013a*; *Kiran et al., 2015*).

Newer vaccine development techniques, such as recombinant DNA technology or viral vector vaccines, may offer advantages in terms of efficacy and safety. Computational vaccinology and *in-silico* prediction of the host's immune response to pathogens/antigens can expedite the development of novel vaccines. Epitope-based vaccines, which target specific antigenic regions of the pathogen, offer a promising approach to vaccine development termed 'reverse vaccinology' due to their potential for inducing targeted immune responses while minimizing side effects (*Rappuoli, 2000*). Computational epitope prediction and immuno-informatics can hasten the design and development of multi-epitope vaccines (*Pizza et al., 2000*; *Masignani, Pizza & Moxon, 2019*). Molecular docking and molecular simulations aid in understanding the binding potential of *in-silico* designed vaccine with host immune cell receptors (*Rappuoli et al., 2016*). Immunoinformatics has been gainfully employed for designing multi-epitope vaccine candidates against KFDV (with a relatively smaller set of genome sequences) and to understand the molecular interactions between the host receptors and virus protein recently (*Arumugam & Varamballi, 2021*; *Dey et al., 2023*; *Hafeez et al., 2023*). The present work is a comprehensive phylogenomic and immunoinformatics analysis of KFDV based on 73 genome sequences to rationally design a multi-epitope vaccine candidate based on a major antigenic protein, which is an envelope protein. Portions of this text were previously published as part of a preprint (https://www.biorxiv.org/content/10.1101/2024.03.14.584963v1).

# MATERIALS AND METHODS

## Study design

The complete genome sequences of the KFDV isolates available with ICMR-National Institute of Virology, Pune, India were analyzed using various bioinformatics tools to determine the lineages and the level of genetic recombination among the isolates. The study aims to design a vaccine candidate that can induce a strong and specific immune response by targeting the envelope protein that plays a key role in the virus-host interaction. However, it is also important to consider the diversity of KFDV strains and the potential for antigenic variation when designing vaccines based on the envelope protein to ensure broad protection. Considering this, various immunoinformatics tools were used in the current study to develop an *in-silico*-designed multi-epitope (B- and T-cell derived) vaccine directed towards the envelope protein of KFDV. The physicochemical properties of the vaccine construct were computed followed by prediction and refinement of its three-dimensional (3D) structure. To analyze the binding affinity and stability, molecular docking analysis and molecular dynamics simulations were performed. Figure 1 shows the different steps for designing the multi-epitope vaccine construct against KFD in our study.

## Next-generation sequencing and phylogenetic analysis

A total of 73 complete genome sequences of KFDV from India were used in this study. Out of these 49 were previously submitted to GenBank by the Indian Council for Medical Research-National Institute of Virology (ICMR-NIV) Pune, and 24 were collected during 2019–2022 and sequenced by the Next generation sequencing approach (Table S1). For next generation sequencing, RNA was extracted from isolates and clinical specimens with a commercially available RNA extraction kit (MagMAX™ Viral/Pathogen; Themo Fisher Scientific, Waltham, MA, USA). The libraries were prepared, pooled, and loaded onto the Illumina platform as per the protocol described earlier (*Yadav et al., 2018*). CLC Genomics software 22.0.2 (Qiagen, Germantown, MD, USA) was used for the sequence analysis. Reference mapping was carried out with the KFDV reference genome (Ref Seq ID: NC_039218) to retrieve the complete genome. Multiple sequence alignment of the KFDV isolates including the reference genome was performed using the tool Multiple Alignment using Fast Fourier Transform (MAFFT) (*Katoh, Rozewicki & Yamada, 2019*). Multiple alignments of individual genes/proteins were also carried out using MAFFT. Molecular Evolutionary Genetic Analysis version 10 (MEGAX) was used for the visualization of genome/gene/protein alignments (*Kumar et al., 2018*). Recombination events were detected using Recombination Detection Program version 4 (RDP4) with $p$-value ≤ 0.005. A sequence is said to be recombinant if predicted by at least three different methods available in RDP4 package (*Martin et al., 2015*). The best nucleotide substitution model was estimated by ModelFinder (*Kalyaanamoorthy et al., 2017*). For the construction of the phylogenetic tree, the maximum likelihood method implemented in Important Quartet based phylogenetic tree (IQTREE) (*Minh et al., 2020*) tool was used. Phylogenetic tree was visualized using Interactive Tree of Life (iTOL) (*Letunic & Bork, 2021*). Molecular clock behavior was tested using TEMPoral Exploration of Sequences and Trees (TempEst)

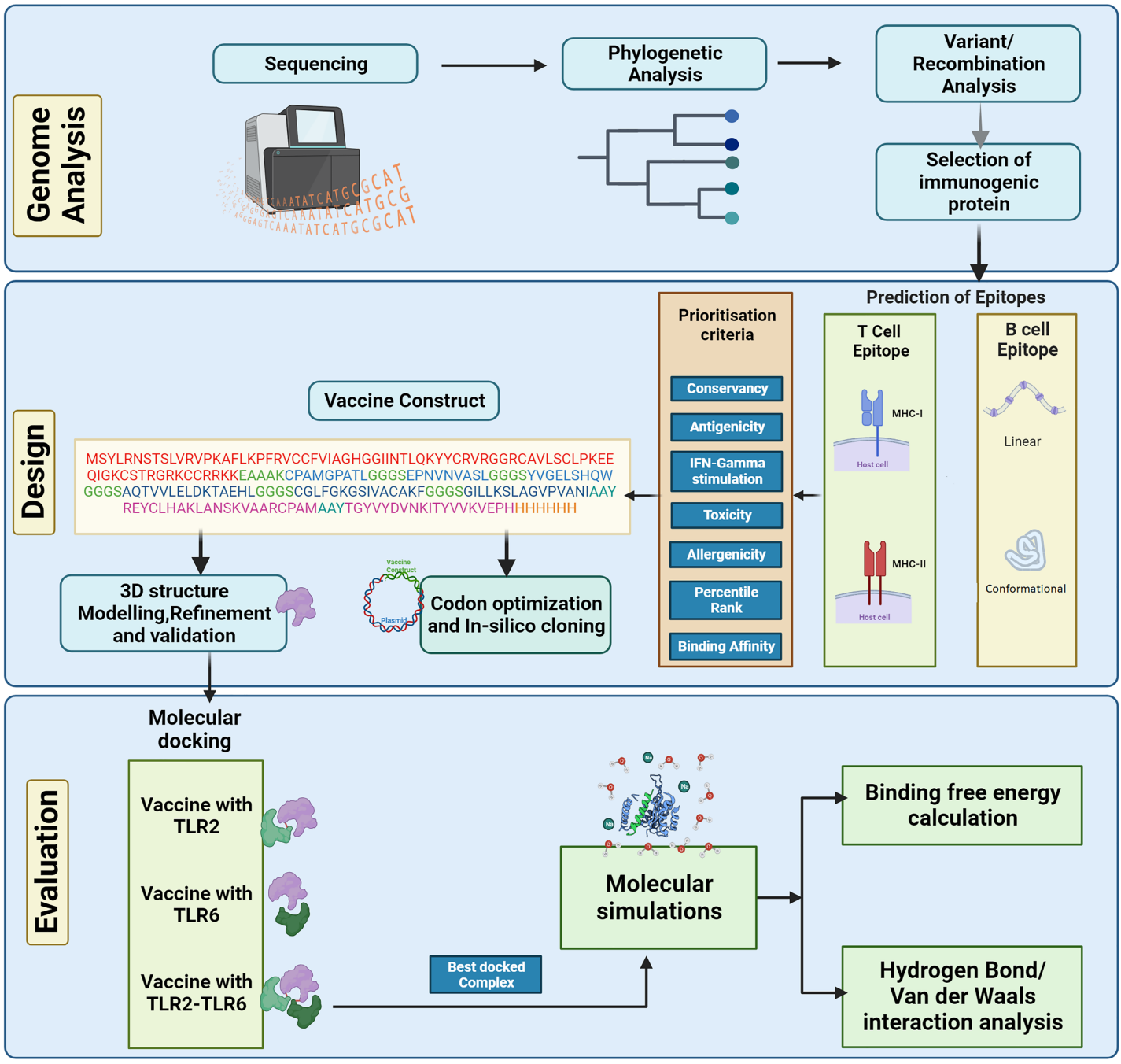


**Figure 1** Schematic representation of steps involved in the *in-silico* design of Kyasanur forest disease vaccine.
Full-size DOI: 10.7717/peerj.18982/fig-1

(*Rambaut et al., 2016*). Bayesian Evolutionary Analysis Sampling Trees (BEAST) v.10.1.4 was used for the estimation of nucleotide substitution rate and lineage divergence (*Suchard et al., 2018*). One billion steps of Markov Chain Monte Carlo (MCMC) were carried out in triplicate. The maximum clade credibility tree was visualized using FigTree (available for download at http://tree.bio.ed.ac.uk/software/figtree/).

## Immunoinformatics analysis

### *T cell epitope prediction*

NetMHCpan EL 4.1 (available at http://tools.iedb.org/mhci/) and NetMHCIIpan 3.2 (available at http://tools.iedb.org/mhcii/) from the IEDB server were used respectively for predicting MHC I and MHC II epitopes (*Reynisson et al., 2020*) with HLA alleles as curated by *Weiskopf et al. (2013)* and *Greenbaum et al. (2011)*. Further filtration of the predicted epitopes was based on MHC binding affinity, percentile rank and by removing largely overlapping epitopes that share the same core region. Computational prediction of IL-4 and IL-10 stimulation has been carried out using IL4Pred (*Dhanda et al., 2013*) and IL-10Pred (*Nagpal et al., 2017*).

### *B-cell epitope prediction*

Prediction of conformational and linear B-cell epitopes was done using Bepipred (available at http://tools.immuneepitope.org/bcell/) and ElliPro (available at http://tools.iedb.org/ellipro/) online tools (*Jespersen et al., 2017*; *Ponomarenko et al., 2008*). For the conservancy of the epitopes in the global isolates, the Epitope Conservancy Analysis tool (available at http://tools.iedb.org/conservancy/) was used (*Bui et al., 2007*). Computational prediction of IFN-gamma stimulation of the predicted epitopes was performed using IFNepitope (*Dhanda, Vir & Raghava, 2013*) (available at https://webs.iiitd.edu.in/raghava/ifnepitope/predict.php). Further prioritization of the predicted epitopes was carried out by testing for antigenicity using Vaxijen 2.0 (*Doytchinova & Flower, 2007*) (available at http://www.ddg-pharmfac.net/vaxijen/). Allergenicity and toxicity testing were done using AllerTopv2.0 (available at https://www.ddg-pharmfac.net/allertop_test/) and ToxinPred (*Dimitrov et al., 2014*; *Gupta et al., 2015*) (available at https://webs.iiitd.edu.in/raghava/toxinpred/), respectively.

### *Construction of multi-epitope vaccine*

The selected T-cell and B-cell epitopes were conjugated with different linkers. The linker regions used were EAAAK, GGGS, and AAY. The N-terminal of the vaccine construct was linked with an adjuvant β-defensin by the EAAAK linker. MHC I and MHC II epitopes were linked by GGGS and the B cell epitopes by AAY. A histidine tag was included at the C terminal of vaccine construct which may be useful during purification steps in experimental validation studies. The use of adjuvant β-defensin would help to enhance the vaccine immunogenicity (*Kim et al., 2018*).

### *Physiochemical properties*

Various physiochemical properties of the vaccine construct were calculated using the online web server ProtParam (*Gasteiger et al., 2005*) (available at https://web.expasy.org/protparam).

### *Prediction of 3D structure of vaccine construct*

The three-dimensional structure of the vaccine construct was predicted using the I-TASSER webserver (*Zhou et al., 2022*). I-TASSER stands for Iterative Threading Assembly Refinement. It develops multiple models, and based on the C-score, the best

model is chosen. The chosen model of the vaccine construct was further refined by molecular dynamics simulations using amberff14SB force field available in AMBER20 simulation package (*Case et al., 2021*). The system preparation was done where the structure was solvated in a water box using the TIP3P model. The system was neutralized by adding charged (18 chloride) ions. The structure was minimized in two stages, namely steepest descent followed by conjugate gradient approaches. Minimization was followed by temperature ramping up to 300 K since the amberff14SB force field (used in this study) with TIP3P water model is parameterized at 300 K (*Maier et al., 2015*). This was followed by an equilibration at NPT condition for one ns, and finally, a production run of 50 ns was carried out. The final model obtained from the simulations was validated by Ramachandran plot analysis using the Procheck webserver (*Laskowski et al., 1993*) (available at https://www.ebi.ac.uk/thornton-srv/software/PROCHECK/).

## Molecular docking with immune cell receptors

The vaccine construct must interact with the host immune cell receptors like Toll-like receptors (TLR) to evoke an immune response. Hence, the binding affinity of TLR2, TLR6 and TLR2-TLR6 receptor complex with the vaccine construct were studied using molecular docking. HADDOCK2.4 webserver (*Dominguez, Boelens & Bonvin, 2003*) (available at https://rascar.science.uu.nl/haddock2.4/) was used for docking studies with TLR2 receptor (PDB ID: 2z7x), TLR6 (PDB ID: 3a79), and TLR2-TLR6 receptor complex (PDB ID: 3a79) (*Dominguez, Boelens & Bonvin, 2003*; *van Zundert et al., 2016*). Chimera software (*Pettersen et al., 2004*) was used for visualization and for removing the hetero water molecules and pam2SCK4 from PDB files. Prior to docking, the active and passive residues were predicted using WHISCY (*De Vries, van Dijk & Bonvin, 2006*) (available at https://wenmr.science.uu.nl/whiscy/). HADDOCK provides multiple docked cluster models. Based on the lowest HADDOCK score, the best-docked cluster was chosen and subjected to molecular dynamics simulations.

## Molecular simulations of TLR2-TLR6-vaccine construct complex

Molecular dynamics simulations were performed for the docked TLR2-TLR6-vaccine construct complex using the AMBER20 simulation package (*Case et al., 2021*). A similar protocol to that of the vaccine construct was followed for the simulations, except that an additional production run of 240 ns was performed. A total of three sets of simulations were performed. Interaction analysis and related statistical analysis were performed for the last 200 ns of simulation data. Root mean square deviation (RMSD), root mean square fluctuation (RMSF), and hydrogen bond analysis were performed using AmberTools21 (*Case et al., 2021*). RMSD indicates how much the structure has deviated from the reference structure. The reference structure considered for the RMSD calculation is the start structure of the simulation. Interaction calculations were performed using the GetContact tool (available at https://getcontacts.github.io/) and the LIGPLOT tool (*Laskowski & Swindells, 2011*). Free energy of binding between the vaccine construct and TLR2-TLR6 receptor, vaccine construct, and TLR2 receptor, and vaccine construct and

TLR6 receptor were computed using the MM-GBSA module of the AMBER20 package. Secondary structure prediction was carried out using PSIPRED4.0 (*Buchan & Jones, 2019*).

### Codon optimization and *in-silico* cloning

Reverse translation and codon optimization was performed using VectorBuilder (https://en.vectorbuilder.com/tool/codon-optimization.html) to achieve a high protein expression level in *E.coli* (strain K12) for future validation studies. The codon-optimized sequence was used for *in-silico* cloning into pET30b (+) using XhoI and NdeI (https://www.snapgene.com/).

## RESULTS

### Analysis of KFDV genomes

There was no evidence of recombination in the KFDV isolates. A linear relationship between root-to-tip distance and time of isolation was observed indicating molecular clock behavior in the dataset (Fig. S1).

### Phylogenetic analysis

Genome-wide nucleotide substitution rate was found to be $4.31 \times 10^{-4}$ (95% HPD: $3.45 \times 10^{-4}$, $5.22 \times 10^{-4}$) substitutions per site per year. Phylogenetic analysis revealed spatio-temporal clustering with few deviations (Fig. 2). Two distinct lineages of KFDV were found, of which, lineage 1 includes isolates sampled from Karnataka during 1957–1972. Lineage 2 was found to demarcate into sub-lineages viz., 2.1 and 2.2. Sub-lineage 2.1 includes isolates from Karnataka and Goa during 2006–2022. Sub-lineage 2.2 further differentiates into 2.2.1 and 2.2.2. It was observed that ten KFDV isolates from Karnataka sampled during 2012–2022 constitute lineage 2.2.1. KFDV strains isolated during 2013–2020 from Maharashtra along with six from Karnataka, two from Goa, and one from Tamil Nadu constitute sub-lineage 2.2.2. Nine representative isolates were identified based on the lineages observed in the phylogenetic tree (Table S2).

### T-cell epitope prediction

MHC class I epitope prediction for envelope protein was carried out for reference HLA alleles as curated by *Weiskopf et al. (2013)*. The predicted epitopes were further filtered based on percentile rank ≤ 1 and predicted binding affinity of 500 nM which resulted in a total of 23 MHC class I epitopes (Table 1). Similarly, MHC class II epitopes were predicted for the HLA reference set curated by *Greenbaum et al. (2011)*. The class II epitopes were prioritized based on removing largely overlapping epitopes that share the same core region, MHC binding affinity IC50 ≤ 1,000 nM, and percentile rank ≤ 10.0 which resulted in a total of 15 MHC class II epitopes (Table 2). Among the short-listed MHC Class II epitopes except epitope 262-GILLKSLAGVPVANI-276, all epitopes were positive for stimulation of both IL-4 and IL-10 (Table S3).

### B-cell epitope prediction

Linear B-cell epitopes were predicted using the envelope protein sequences of the nine representative KFDV isolates which were further prioritized based on their conservancy

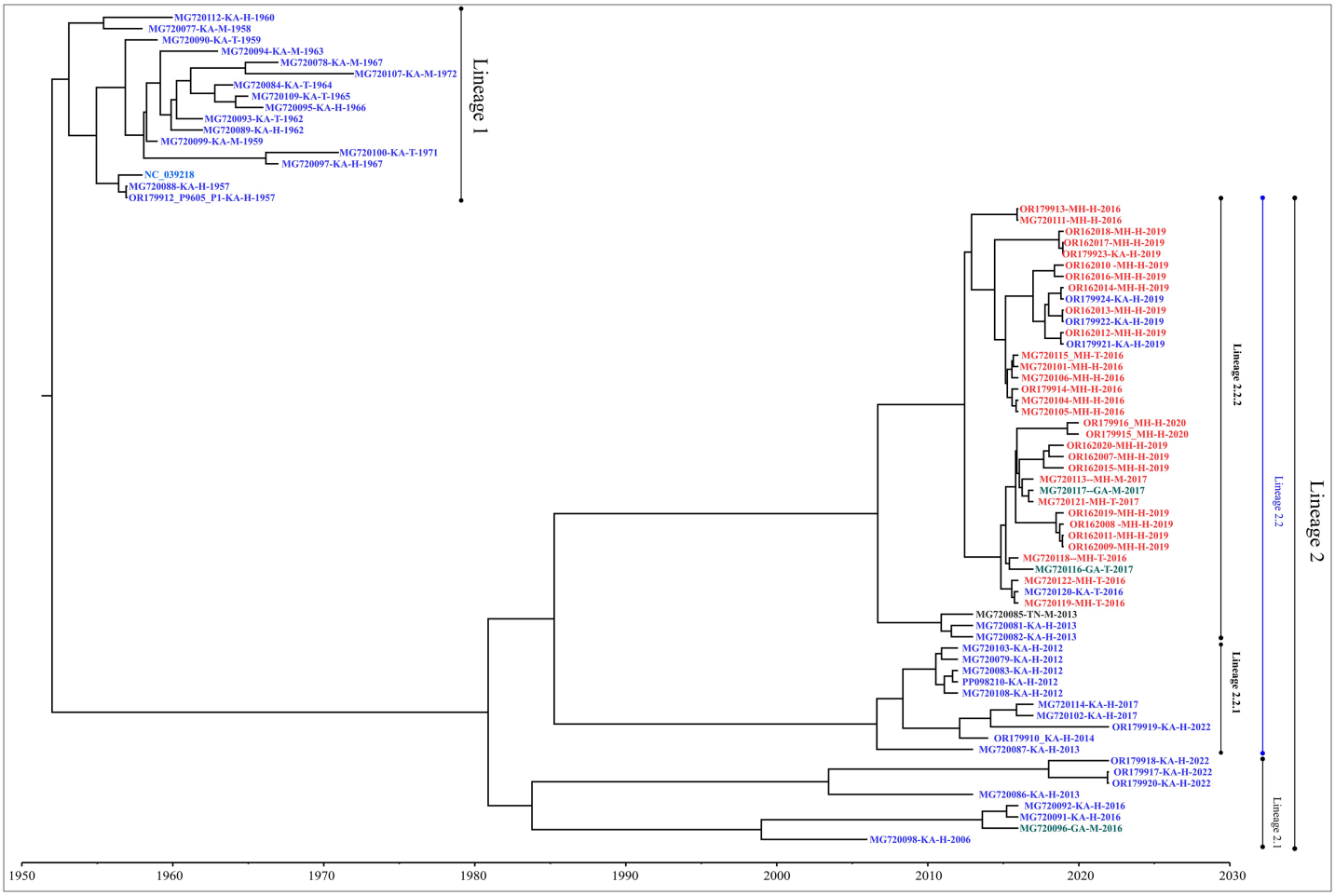


**Figure 2** **Maximum clade credibility tree of KFDV derived using complete genome.** Full-size DOI: 10.7717/peerj.18982/fig-2

across all global KFDV isolates, the ability to induce IFN-Gamma stimulation, and antigenicity (Table 3). The predicted 3D structure of envelope protein was used for conformational epitope prediction and three epitopes were prioritized based on similar criteria as described above for linear B-cell epitopes (Table 4).

## Construction of multi-epitope vaccine candidate

The prioritized epitopes were combined with the help of different linkers, β-defensin adjuvant, and histidine tag. The length of the final vaccine construct is 226 amino acids with a molecular weight of 23.09 kDa (Fig. 3). The vaccine construct has a theoretical pI value of 9.54, suggesting its alkaline nature and the estimated half-life is 30 h (mammalian reticulocytes, *in-vitro*). The computed instability index (II) was found to be 39.08 which classifies the protein as stable. The average hydropathicity was around −0.029, indicating the hydrophilic nature of the vaccine construct.

**Table 1** List of short-listed MHC-Class I epitopes belonging to the envelope protein of KFDV.

| Epitope | Position | IFN-Gamma | Antigenicity | Percent of protein sequence matches at identity <= 100% | Rank | IC50 |
|---|---|---|---|---|---|---|
| STIGRVLEK | 397–405 | Positive | Non-antigen | 100.00% (74/74) | 0.01 | 21,121.52 |
| KAWQVHRDW | 211–219 | Positive | Non-antigen | 100.00% (74/74) | 0.01 | 9,711.53 |
| LTVVGEHAW | 413–421 | Negative | Antigen | 98.65% (73/74) | 0.01 | 19,183.08 |
| YVGELSHQW | 384–392 | Positive | Antigen | 98.65% (73/74) | 0.01 | 69.87 |
| FLPRILLGV | 454–462 | Negative | Non-antigen | 100.00% (74/74) | 0.04 | 14,056.58 |
| ILLKSLAGV | 263–271 | Positive | Non-antigen | 100.00% (74/74) | 0.05 | 21,522.7 |
| TRASLVLEL | 19–27 | Positive | Antigen | 2.70% (2/74) | 0.01 | 21,522.7 |
| KLKMKGMTY | 296–304 | Negative | Antigen | 100.00% (74/74) | 0.01 | 15,983.96 |
| ASFTTQSEK | 163–171 | Negative | Antigen | 100.00% (74/74) | 0.01 | 17,634.96 |
| LPPGDNIIY | 376–384 | Negative | Non-antigen | 100.00% (74/74) | 0.04 | 17,158.59 |
| QEWNHANRL | 233–241 | Negative | Antigen | 48.65% (36/74) | 0.04 | 24,903.62 |
| TRVSLVLEL | 19–27 | Positive | Antigen | 97.30% (72/74) | 0.01 | 19,937.05 |
| VYDVNKITY | 131–139 | Negative | Non-antigen | 100.00% (74/74) | 0.01 | 11,777.84 |
| NHADRLVEF | 236–244 | Negative | Non-antigen | 51.35% (38/74) | 0.01 | 1,969.83 |
| CPAMGPATL | 74–82 | Positive | Antigen | 100.00% (74/74) | 0.03 | 27.6 |
| VEFGEPHAV | 242–250 | Positive | Antigen | 100.00% (74/74) | 0.01 | 27,602.87 |
| EPNVNVASL | 349–357 | Positive | Antigen | 100.00% (74/74) | 0.03 | 256.83 |
| EHLPKAWQV | 207–215 | Negative | Non-antigen | 100.00% (74/74) | 0.02 | 25,442.61 |
| KMKGMTYTV | 298–306 | Negative | Non-antigen | 100.00% (74/74) | 0.02 | 7,773.82 |
| VANIEGSKY | 273–281 | Negative | Non-antigen | 95.95% (71/74) | 0.05 | 7,450.51 |
| NHANRLVEF | 236–244 | Negative | Non-antigen | 48.65% (36/74) | 0.02 | 19,651.14 |
| LQLPPGDNI | 374–382 | Negative | Non-antigen | 100.00% (74/74) | 0.03 | 26,164.55 |
| FGEPHAVKM | 244–252 | Negative | Non-antigen | 100.00% (74/74) | 0.02 | 19,680.08 |

**Note:**
Epitopes used in the design of vaccine construct are underlined.

## Prediction of 3D structure, refinement, and validation

For the prediction of tertiary structure, the I-TASSER server was used. The server predicted five models, and based on the C-score, the top-scoring model was selected for further refinement. I-TASSER generates three dimensional atomic structure based on the multiple threading alignments and iterative structural assembly simulations. The threading templates PDB IDs (%identity) used were 3p54 (19%), 7cth (16%), 7esd (20%), 2i69 (23%), 6epk (20%), 4fg0 (22%), 7w6b (8%) and 1svb (20%). The structure was refined with the help of molecular dynamics simulations. The structural quality of the predicted and refined vaccine 3D structure was validated by the Ramachandran plot (Fig. S2). ~98.4% of amino acids belong to the most favored, additional allowed, and generously allowed regions. Three residues, *i.e.*, 1.6%, belonged to the disallowed region. Overall, the model was observed to have good quality with predicted Z score of −3.54 using ProSA analysis (*Sippl, 1993*).

**Table 2** List of short-listed MHC-Class II epitopes belonging to the envelope protein of KFDV.

| Epitope | Position | IFN-Gamma | Antigenicity | Percent of protein sequence matches at identity <= 100% | Rank | ic50 |
|---|---|---|---|---|---|---|
| AQTVVLELDKTAEHL | 195–209 | Positive | Antigen | 98.65% (73/74) | 9.3 | 30.7 |
| AVAHGEPNVNVASLI | 344–358 | Positive | Antigen | 100.00% (74/74) | 9.9 | 98.5 |
| CGLFGKGSIVACAKF | 105–119 | Positive | Antigen | 100.00% (74/74) | 1.6 | 25.3 |
| DQTGILLKSLAGVPV | 259–273 | Positive | Antigen | 100.00% (74/74) | 1.21 | 6.9 |
| EFGEPHAVKMDIFNL | 243–257 | Negative | Non-antigen | 100.00% (74/74) | 7.5 | 123 |
| EGKPSVDVWLDDIHQ | 36–50 | Positive | Antigen | 100.00% (74/74) | 2.8 | 280.1 |
| EKTILTLGDYGDISL | 170–184 | Negative | Non-antigen | 94.59% (70/74) | 6.4 | 357.7 |
| GHDTVVMEVTYTGSK | 322–336 | Positive | Antigen | 100.00% (74/74) | 8.6 | 197.5 |
| GIERLTVVGEHAWDF | 409–423 | Negative | Non-antigen | 98.65% (73/74) | 7.8 | 726.2 |
| GILLKSLAGVPVANI | 262–276 | Positive | Antigen | 100.00% (74/74) | 0.38 | 3.4 |
| LPKAWQVHRDWFEDL | 209–223 | Positive | Antigen | 100.00% (74/74) | 7.4 | 101.5 |
| PGDNIIYVGELSHQW | 378–392 | Negative | Non-antigen | 98.65% (73/74) | 8.8 | 312.5 |
| REYCLHAKLANSKVA | 57–71 | Positive | Antigen | 100.00% (74/74) | 2.8 | 15.8 |
| RKTASFTTQSEKTIL | 160–174 | Positive | Antigen | 100.00% (74/74) | 9.5 | 849.5 |
| SGTQGTTRASLVLEL | 13–27 | Negative | Non-antigen | 2.70% (2/74) | 8.2 | 38.6 |

**Note:**
Epitopes used in the vaccine construct are underlined.

**Table 3** List of predicted linear B-cell epitopes belonging to the envelope protein of KFDV.

| Epitope sequence | Epitope length | Position | IFN-Gamma | Antigenicity | Percent of protein sequence matches at identity <= 100% |
|---|---|---|---|---|---|
| REYCLHAKLANSKVAARCPAM | 21 | 57–77* | Yes | Yes | 100.00% (74/74) |
| EHLPKAWQVHRD | 12 | 206–218* | No | No | 100.00% (74/74) |
| GILLKSLAGVPVANI | 15 | 262–276 | No | No | 100.00% (74/74) |
| SKPCRIPVRAVAHGE | 15 | 334–349 | No | Yes | 100.00% (74/74) |
| DISLTCRVTSGVDPAQTVVLELD | 23 | 180–203 | No | Yes | 97.30% (72/74) |
| FGGVGFLPRILLGVALAWLG | 20 | 448–468* | No | Yes | 95.95% (71/74) |
| TGYVYDVNKITYVVKVEPH | 19 | 127–146 | Yes | Yes | 100.00% (74/74) |
| SKYHLQSGHVTCDVGLE | 17 | 279–295 | No | Yes | 95.95% (71/74) |
| GGMLSSVGKALHTAFGA | 17 | 425–443 | Yes | Yes | 81.08% (60/74) |
| RVSLVLELGGCVTLT | 15 | 19–34 | No | Yes | 97.30% (72/74) |
| KGSIVACAKFSCE | 13 | 108–122* | No | Yes | 95.95% (71/74) |
| NIIYVGELSHQW | 12 | 380–392 | No | Yes | 98.65% (73/74) |

**Note:**
Epitopes short-listed to design vaccine construct are underlined. Asterisk indicates experimentally validated epitopes in other *Flavivirus* members (*Fumagalli, Figueiredo & Aquino, 2021*).

## Docking of vaccine construct with host receptors (TLR2, TLR6, and TLR2-TLR6 complex)

Docking of vaccine construct was performed with individual TLRs (TLR2 and TLR6) as well as TLR2-TLR6 complex. Table 5 shows the statistics for the refined model with TLR2,

**Table 4** List of predicted conformational B-cell epitopes belonging to the envelope protein of KFDV.

| Epitope | Epitope length | Position | IFN-Gamma | Antigenicity | % of protein sequence matches at identity <= 100% | Score |
|---|---|---|---|---|---|---|
| LEKLKMKGMTYTVCEGSKFAWKRPPT | 26 | 294–319 | Yes | No | 100.00% (74/74) | 0.704 |
| LPPGDNIIYVGELSHQWFQKGSTIG | 25 | 376–400 | No | Yes | 100.00% (74/74) | 0.7 |
| PSMETTGGG | 9 | 362–370 | No | Yes | 98.65% (73/74) | 0.685 |
| EGAQEW | 6 | 230–235 | Yes | No | 98.65% (73/74) | 0.583 |
| TTQSEKTILTLGDYGD | 16 | 166–181 | No | Yes | 100.00% (74/74) | 0.568 |
| VGGMLSSVGKALHTAFGAA | 19 | 426–444 | No | Yes | 100.00% (74/74) | 0.644 |
| LPRILLGVALAWLGLNSRNPTLSVGFLITGGLVL | 34 | 455–488 | No | Yes | 100.00% (74/74) | 0.845 |
| HAKLANSKVAARCPA MGPATLPEEHQASTV CRRDQSDRGWGNHC GLFGKGSIVACAKFSCETK | 63 | 62–124 | Yes | Yes | 100.00% (74/74) | 0.81 |
| EFGEPHAVKMDIFNL | 15 | 243–257 | No | No | 100.00% (74/74) | 0.767 |
| MEVTYTGSKPCRIPVRAVAHGEPNVNVA | 28 | 328–355 | No | Yes | 100.00% (74/74) | 0.709 |
| TQGTTR | 6 | 15–20 | No | No | 100.00% (74/74) | 0.565 |

**Note:**
Epitopes short-listed to design vaccine-construct are underlined.

TLR6, and TLR2-TLR6 complex. As TLR2 is known to form heterodimer with TLR6, docking with this complex was further investigated. Docking of TLR2-TLR6 complex with vaccine construct (Figs. 3B and 3C) resulted in 73 structures that group into 10 cluster(s). These represent 36.5% of the generated water-refined models. The top cluster was considered the most reliable based on the HADDOCK score. Further refinement of a representative model of the top cluster resulted in nine structures that are 100% water-refined models. The proximity between the vaccine construct and TLR receptors is indicated by a buried surface area of 4,564.2 +/− 299.3 $Å^2$. The RMSD of the docked complex is around 0.6 +/− 0.2, further reiterating the model's good quality (*Poli, Martinelli & Tuccinardi, 2016*; *Boittier et al., 2020*; *Collins et al., 2024*).

## Molecular simulations of TLR2-TLR6-vaccine construct

The stability of the binding between TLR2-TLR6-vaccine construct was assessed by calculating distances between amino acid residues belonging to vaccine construct, TLR2 and TLR6 (Figs. S3A and S3B). The figure clearly depicts that the distance is maintained for most of the simulation time indicating stable binding of vaccine construct with TLR2-TLR6. RMSD for the entire complex and individual proteins, *i.e.*, TLR2, TLR6 receptors, and vaccine construct, were computed (Fig. 4). The RMSD value for the entire protein lies in the range of 4 to 5 Å. For the TLR2 and TLR6 receptors, it is in the range of 2 to 3 Å, and for the vaccine construct, it is in the range of 6 to 7 Å. This clearly shows that the RMSD values tend to stabilize over time, indicating equilibration of the system. The higher RMSD value in vaccine construct may be attributed to the loop regions. Further, to inspect which regions of the vaccine construct show higher fluctuations, RMSF was calculated for the vaccine construct (Fig. 5). From Fig. 5, it can be observed that the region which lie in

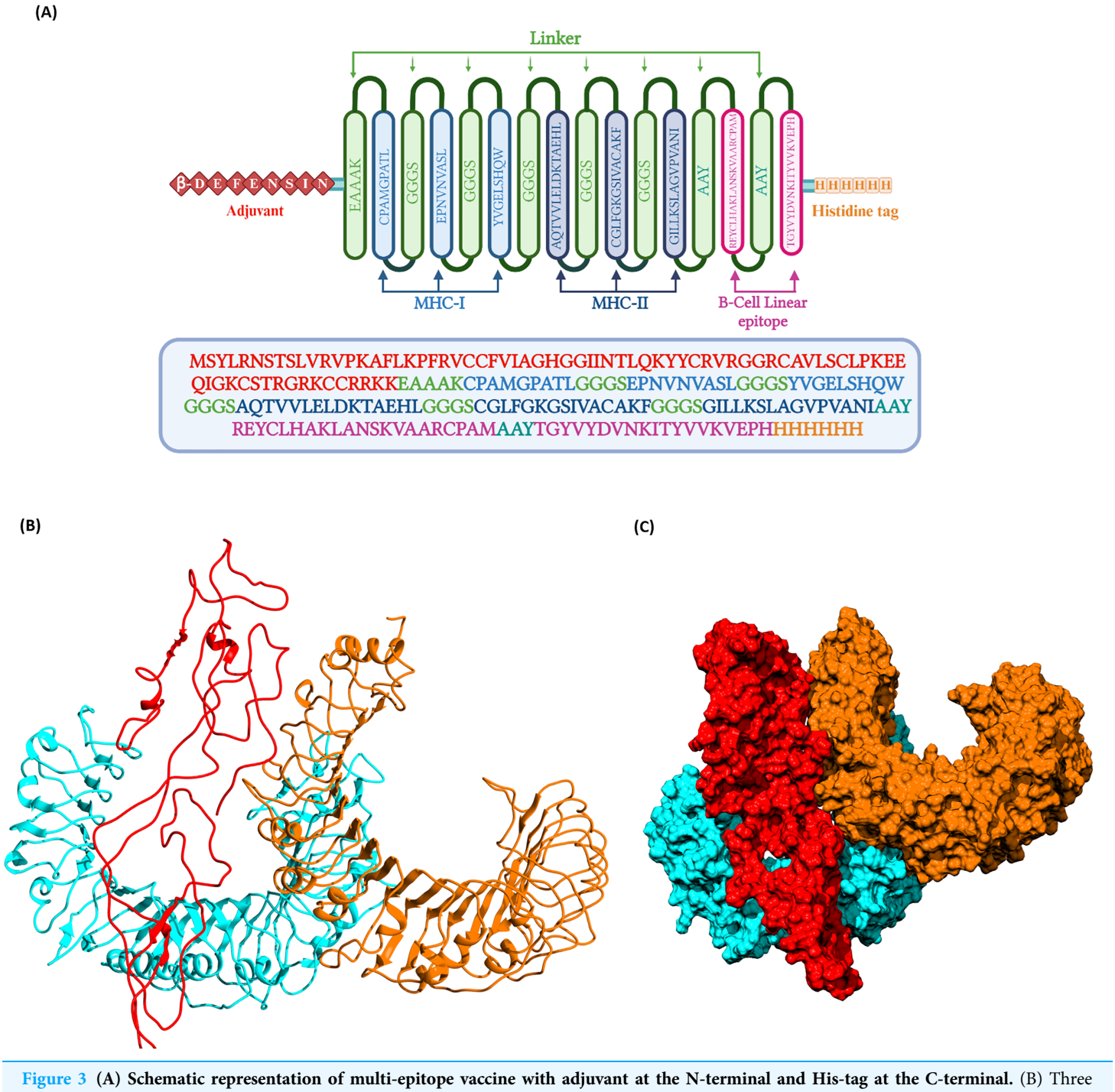


**Figure 3 (A) Schematic representation of multi-epitope vaccine with adjuvant at the N-terminal and His-tag at the C-terminal.** (B) Three dimentional structure of the docked complex comprising KFDV vaccine construct with human receptor complex of TLR2-TLR6 shown in ribbon model. (C) Three dimentional structure of the docked complex shown as space-filled model. Color code: Vaccine construct is depicted in red, TLR6 is in blue, and TLR2 is shown in orange.
Full-size DOI: 10.7717/peerj.18982/fig-3

**Table 5** Statistical parameters for interaction between vaccine construct with TLR2, TLR6, and TLR2-TLR6 complex.

| Parameter | TLR2 | TLR6 | TLR2-TLR6 |
|---|---|---|---|
| HADDOCK score | −20.2 +/− 3.8 | −82.8 +/− 37.2 | −13.0 +/− 9.3 |
| Cluster size | 19 | 9 | 9 |
| RMSD from the overall lowest-energy structure | 0.8 +/− 0.1 | 1.4 +/− 1.0 | 0.6 +/− 0.2 |
| Van der Waal's energy (kcal/mol) | −124.0 +/− 19.1 | −146.2 +/− 11.1 | −117.8 +/− 14.8 |
| Electrostatic energy (kcal/mol) | −302.0 +/− 49.0 | −501.1 +/− 63.6 | −526.7+/− 32.8 |
| Desolvation energy (kcal/mol) | −36.8 +/− 6.2 | −10.9 +/− 3.8 | −9.2 +/− 6.2 |
| Restraints violation energy (kcal/mol) | 2,009.5 +/− 219.22 | 1,745.3 +/− 162.66 | 6,996.5 +/− 225.43 |
| Buried surface area | 3,996.0 +/− 365.4 | 4,874.8 +/− 323.6 | 4,564.2 +/− 299.3 |
| Z-Score | −2.3 | −2.1 | −2 |

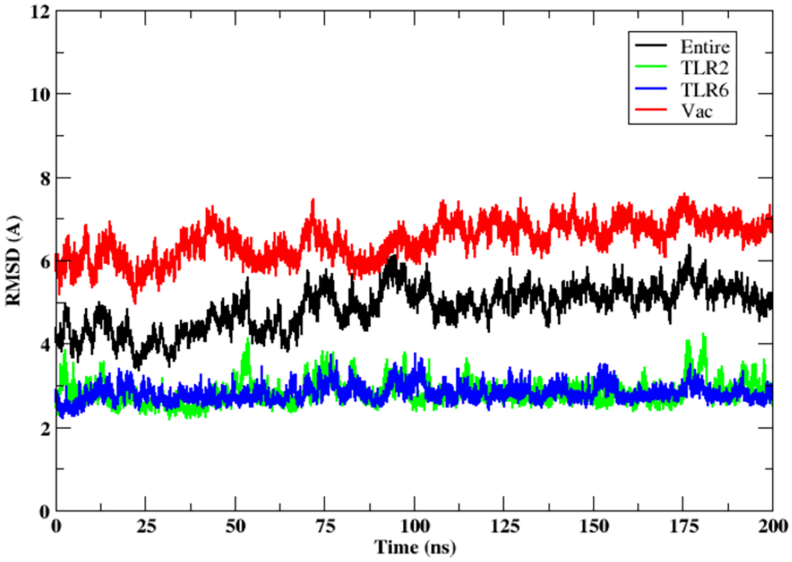


**Figure 4** RMSD of the 3D structure of vaccine construct with TLR2-TLR6 docked complex. RMSD of the entire complex (black), vaccine construct (red), TLR2 receptor (green) and TLR6 receptor (blue). Full-size DOI: 10.7717/peerj.18982/fig-4

residue range of 80–100 and 130–150 show higher fluctuations. Two replicates (two and three) show similar trends for RMSD and RMSF distribution (Figs. S4 and S5).

GetContact tool was used for the calculation of hydrogen bonds and Van der Waal's interactions between vaccine construct and TLR2–TLR6. All the hydrogen bonds and Van der Waal's interactions having occupancy of ≥20% have been shown in Tables S4, S5 and Figs. S6, S7. TLR2 forms eleven hydrogen bonds with the vaccine construct. Among these, four hydrogen bonds are between the epitope regions and TLR2, and the remaining seven hydrogen bonds are between the linker region or β-defensin region and TLR2. Besides hydrogen bonds, the vaccine construct formed thirty-eight Van der Waal's interactions with TLR2. Of these, twenty-six interactions were between epitope regions of the vaccine construct and TLR2. Similarly, TLR6 formed twenty-six hydrogen bonds and sixty-two Van der Waal's interactions with the vaccine construct. Of the twenty-six hydrogen bonds,

seven were between epitope regions and TLR6; fourteen were between the adjuvant and the TLR6. Similarly, of the sixty-two Van der Waal's interactions, twenty-five involved epitope regions. Thus, the TLR6 receptor has maximum number of interactions with vaccine construct as compared to TLR2.

Further, the free energy of binding between different components of the complex, namely, vaccine construct-TLR2/TLR6, vaccine construct and TLR2-TLR6 complex, and between TLR2-TLR6, were computed and are shown in Fig. 6. It can be observed that the vaccine construct shows strong free energy of binding with TLR2-TLR6 complex with values around −80 to −100 kcal/mol. Among the two TLRs, the vaccine construct showed better binding free energy with TLR6 as compared to TLR2. The vaccine construct and TLR2 binding free energy lies in the range of −25 to −27 kcal/mol, while it lies in the range of −60 to −75 kcal/mol for the vaccine construct and TLR6. The free energy of binding between two TLRs lies in the range of 0 to 5 kcal/mol, which indicates weak binding. Replicate two and replicate three show similar trends for free energy of binding (Fig. S8).

### Codon optimization and *in-silico* cloning

Vector Builder was used for codon optimization in the *Escherichia coli* (strain K12) expression system. The GC content was 59.43% and Codon Adaptation Index (CAI) was 0.95. A codon-optimized sequence of vaccine construct was used for *in-silico* insertion into pET30b (+) between XhoI and NdeI restriction sites (Fig. 7).

## DISCUSSION

Kyasanur forest disease is spreading to newer areas. Vaccination has been one of the primary preventive measures. However, the efficacy of the existing vaccine may vary, and it is crucial to boost its effectiveness or develop new vaccines with improved efficacy. A highly immunogenic vaccine is required to fight against this disease and its rapid dispersal to newer areas. The availability of genomic data and immunoinformatics tools aid in development of epitope-based vaccines that can be screened in an efficient manner. Many effective vaccines against infectious diseases designed using reverse vaccinology approaches (that rely on immunoinformatics tools) have been experimentally validated (*Pizza et al., 2000*; *Masignani, Pizza & Moxon, 2019*; *Ismail, Ahmad & Azam, 2020*).

Different research groups have gainfully utilised computational vaccine design approaches for predicting B- and T-cell epitopes to enhance the pace of vaccine development (*Pizza et al., 2000*; *Masignani, Pizza & Moxon, 2019*; *Arumugam & Varamballi, 2021*; *Dey et al., 2023*; *Hafeez et al., 2023*). We have analyzed genome sequences isolated during 1957–2022, and it was noted that there is no evidence of genetic recombination among the isolates.

In this study, the envelope protein of KFDV was chosen to design a multi-epitope vaccine candidate. Previous studies conducted on KFDV demonstrated the suitability of the envelope protein as a candidate for new vaccines and diagnostics (*Dey et al., 2023*). The envelope protein is responsible for the entry of the virus into the host cells by receptor binding and fusion of viral and cellular membranes (*Trapido et al., 1959*). The Ecto-domain-III (EIII) of the envelope protein of flaviviruses evokes neutralizing epitopes (*Liu*

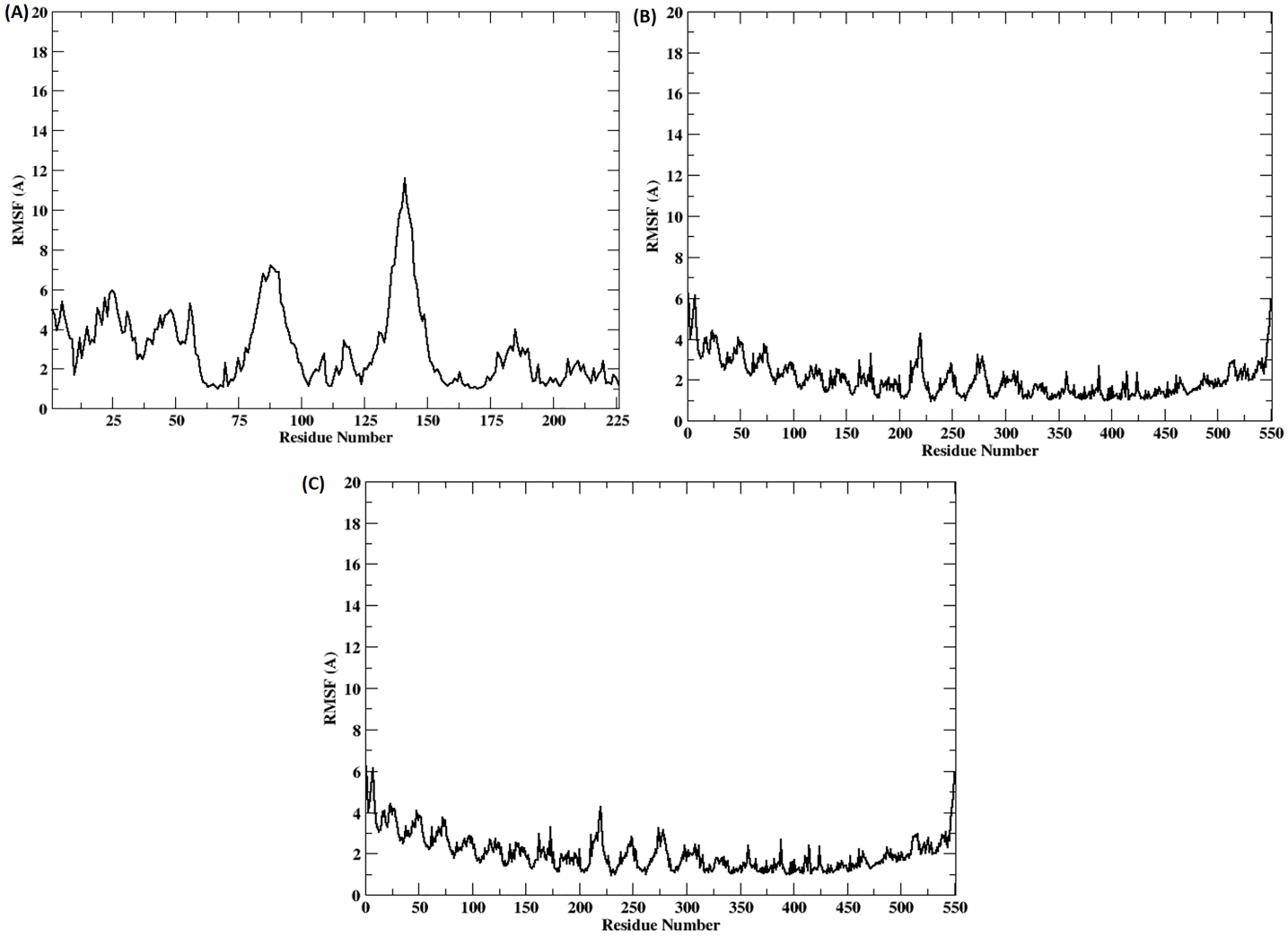


**Figure 5 (A–C) RMSF of the vaccine construct docked with (A) TLR-2 (B) TLR6 (C) TLR2-TLR6 receptor complex.**
Full-size DOI: 10.7717/peerj.18982/fig-5

*et al., 2015*). In earlier studies on immune response, a notable B- and T-cell response was observed in KFDV-infected patients (*Devadiga et al., 2020*). This suggests the need to develop a potential vaccine for KFD that can elicit both humoral and cellular immune responses. Different immunoinformatics tools were used for the prediction and prioritization of a set of B-cell and T-cell (MHC I, and MHC II) epitopes. MHC class I and MHC class II epitopes of envelope protein were predicted using HLA reference alleles. MHC molecules present the peptide epitopes to the T-cell receptors (TCR). MHC I present the peptides to cytotoxic T lymphocytes through the cytosolic pathway and MHC II to the helper T lymphocytes through the endocytic pathway. The non-allergen, non-toxic, IFN-positive epitopes that can stimulate IL-4 and IL-10 cytokines (for MHC-II epitopes) were selected for the final vaccine construct. We designed the multi-epitope vaccine construct by joining the selected predicted epitopes using linkers. There are many *in-silico* multi-epitope vaccine candidates for KFDV and other infectious diseases (*Hafeez et al.,*

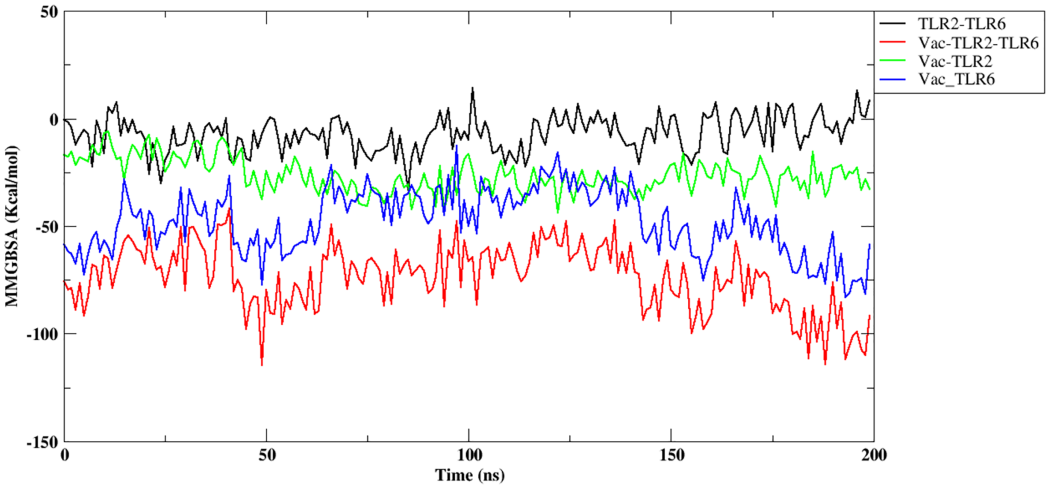


**Figure 6** **Free energy of binding between vaccine construct and TLR2-TLR6 complex. TLR2 and TLR6 (black), vaccine construct and TLR2-TLR6 complex (red), vaccine construct and TLR2 (green), vaccine construct and TLR6 (blue).** Full-size DOI: 10.7717/peerj.18982/fig-6

*2023*; *Ikram et al., 2023*; *Naz et al., 2020*, *2023*). The glycosylation pattern of the epitope has effects on the immunogenicity of the vaccine (*Dowling et al., 2007*; *Singh et al., 2020*). The prioritized epitopes were compared with the key amino acids of the envelope protein. One of the selected epitopes 57-REYCLHAKLANSKVAARCPAM-77 contains the Asp67. The N-glycosylation of the Asp67 of E-protein is responsible for the dengue viral assembly or exit and dendritic cell infection by interacting with DC-SIGN receptors (*Pokidysheva et al., 2006*). In the studies conducted by *Dey et al. (2023)* Asp67 of E-protein in KFDV was predicted to play a role in viral recognition and infection. The ecto-domain-III (EIII) contains the receptor binding region of the envelope protein. The amino acids that form the receptor binding regions are K315, L388, H390, Q391, K395, and F398 (*Dey et al., 2023*). The epitope 384-YVGELSHQW-392 of the vaccine construct includes L388, H390, and Q391 that are likely to enhance the receptor binding ability of the multi-epitope vaccine. Usually, the purified proteins or peptides are less immunogenic, so there is a need to add an adjuvant at the terminal of the peptide to enhance immunogenicity. To increase the immunogenicity of the vaccine construct, β-defensin adjuvant was added (*Kim et al., 2018*) at the N-terminal end along with His tag at the C-terminal end which may aid in purification of the protein in future experimental validation studies. Toll-like receptors (TLR) recognize the microbial components and elicit immune responses by inducing innate immunity followed by adaptive immunity (*Barton, 2007*; *Xagorari & Chlichlia, 2008*; *Zheng et al., 2021*). Many studies have reported the role of TLR2 as a host receptor for the envelope protein to evoke the innate immune response (*Zheng et al., 2021*). TLR2 is the most ubiquitous and is the only TLR that can form heterodimers with more than two other types of TLRs. It forms a heterodimer with TLR6. It interacts with a large number of other non-TLR molecules, thereby increasing its capacity to recognize pathogen-associated molecular patterns (PAMPs) (*Zähringer et al., 2008*). The activation of the TLR2-TLR6 heterodimer initiates a cascade of immune responses that play a dual role in antiviral defense. Depending on the context and extent of activation, this signaling can either inhibit


**Figure 7** ***In-silico*** **cloning of multi-epitope vaccine in pET30b (+).** The red color represents the epitope vaccine sequence inserted between NdeI and XhoI. Full-size DOI: 10.7717/peerj.18982/fig-7

viral replication or promote inflammation and tissue damage. The NS1 protein of dengue virus (DV) has been identified as a critical ligand that activates this receptor complex, leading to an upregulation of pro-inflammatory cytokines, including IL-6 and TNF-alpha (*Chen, Ng & Chu, 2015*). However, evidence from studies conducted by *Modhiran et al. (2017)* suggests that TLR4, rather than the TLR2-TLR6 heterodimer, mediates this activation. Beyond DV, the TLR2-TLR6 pathway also contributes to the innate immune response against respiratory syncytial virus (RSV), indicating its broader relevance in antiviral defense mechanisms (*Murawski et al., 2009*). TLR2 also interacts with molecules like human β-defensin-3, heat shock proteins, and high mobility group box 1 protein and considers them as endogenous ligands (*Funderburg et al., 2007*). We have used the β-defensin as an adjuvant, which can be recognized by TLR2-TLR1 and TLR2-TLR6 heterodimers, increasing the interactive ability of the vaccine construct with the TLR. The heterodimerization increases the range of recognizable motifs by the receptors. In previous

studies of KFDV multi-epitope vaccine, molecular docking was done only with TLR2 (*Arumugam & Varamballi, 2021*; *Hafeez et al., 2023*), which is a major limitation as TLR2 also recognizes the viral proteins in their heterodimeric forms (*Cuevas & Ross, 2014*). Thus, in the present study, the ability of the TLR2 to form a heterodimer with TLR6 was considered, and the vaccine construct was docked with TLR2-TLR6 complex. The docking and simulation study showed that the epitope regions of the vaccine construct formed hydrogen bonds and Van der Waals interactions with both TLR2 and TLR6 and most of the interactions were stable throughout the simulation time. Further, the MM-GBSA results also showed strong free energy of binding of vaccine construct with the TLR2-TLR6 complex. Thus, the study indicates that the vaccine construct forms a stable complex with TLR2-TLR6.

Codon optimization was done to enhance the translation efficiency in *E. coli* (Strain K12). The GC content of 59.43% (30–70%) and CAI 0.95 (0.8–1.0) obtained were in the optimum range for protein expression in the target organism.

### Limitations of the study

It needs to be mentioned that in the present study, only the major antigenic protein, namely envelope protein, was used in the design of multi-epitope vaccine candidate. The inclusion of other structural (capsid and membrane) and non-structural (NS1-NS5) viral proteins would provide a more comprehensive immune response. The placement of predicted B- and T-cell epitopes in the vaccine construct is also known to play a role in eliciting the desired immunogenicity; hence, different arrangements of the epitopes need to be verified. Prediction of MHC-I/II and their binding with epitopes promises to provide a more rigorous criterion for epitope prioritization and hence is proposed to be carried out in future studies. Molecular docking studies of the vaccine construct with other TLRs would also enable a comparative analysis of the binding energies.

## CONCLUSION

The current work describes the comprehensive computational analysis of 73 complete genome sequences of KFDV (1957–2022). The goal is to design of an immunoinformatics-based multi-epitope vaccine against KFDV considering predicted T- and B-cell epitopes and represents a proactive approach to address this emerging infectious disease. Molecular docking and simulations of the vaccine construct with TLR2-TLR6 complex indicate stable binding. Further research, including *in-vitro* and *in-vivo* studies, will be necessary to validate the vaccine's efficacy, safety, and potential for clinical use.

## ACKNOWLEDGEMENTS

The authors gratefully acknowledge the encouragement and support extended by Dr. Sheela Godbole. We also acknowledge the excellent support from Dr. Abhinendra Kumar, Mr. Rajen Lakra, Mr. Prasad Sarkale, Mr. Hitesh Dighe, Mr. Deepak Mali, Ms. Pranita Gawande, Ms. Ujjwala Gaikwad, Ms. Kumari Vaishnavi and Mrs. Pratiksha Vedapathak. The authors acknowledge the computing infrastructure provided by Bioinformatics

Resources and Applications Facility (BRAF), Centre for Development of Advanced Computing, Pune.

## ADDITIONAL INFORMATION AND DECLARATIONS


### Funding

The grant was provided by the Indian Council of Medical Research, New Delhi, India under the extramural project 'Sustainable laboratory network for monitoring of Viral Hemorrhagic Fever viruses in India and enhancing bio-risk mitigation for High risk group pathogen' with the grant number: VIR/28/2020/ECD-1 dated 10.05.2023. The funders had no role in study design, data collection and analysis, decision to publish, or preparation of the manuscript.

### Grant Disclosures

The following grant information was disclosed by the authors:
Indian Council of Medical Research, New Delhi, India: VIR/28/2020/ECD-1.


### Competing Interests

The authors declare that they have no competing interests.

### Author Contributions

- Sunitha Manjari Kasibhatla conceived and designed the experiments, performed the experiments, analyzed the data, prepared figures and/or tables, authored or reviewed drafts of the article, and approved the final draft.
- Lekshmi Rajan performed the experiments, prepared figures and/or tables, authored or reviewed drafts of the article, and approved the final draft.
- Anita Shete performed the experiments, authored or reviewed drafts of the article, and approved the final draft.
- Vinod Jani performed the experiments, analyzed the data, prepared figures and/or tables, authored or reviewed drafts of the article, and approved the final draft.
- Savita Yadav performed the experiments, analyzed the data, prepared figures and/or tables, authored or reviewed drafts of the article, and approved the final draft.
- Yash Joshi performed the experiments, analyzed the data, prepared figures and/or tables, authored or reviewed drafts of the article, and approved the final draft.
- Rima Sahay performed the experiments, authored or reviewed drafts of the article, and approved the final draft.
- Deepak Y. Patil performed the experiments, authored or reviewed drafts of the article, and approved the final draft.
- Sreelekshmy Mohandas performed the experiments, authored or reviewed drafts of the article, and approved the final draft.
- Triparna Majumdar performed the experiments, authored or reviewed drafts of the article, and approved the final draft.
- Uddhavesh Sonavane performed the experiments, analyzed the data, prepared figures and/or tables, authored or reviewed drafts of the article, and approved the final draft.

- Rajendra Joshi conceived and designed the experiments, performed the experiments, authored or reviewed drafts of the article, and approved the final draft.
- Pragya Yadav conceived and designed the experiments, performed the experiments, authored or reviewed drafts of the article, and approved the final draft.

## DNA Deposition

The following information was supplied regarding the deposition of DNA sequences:

The KFDV sequences are available at GenBank: MG720114, OR162010, MG720091, OR162020, MG720116, OR179916, OR162012, OR162018, MG720114.

## Data Availability

The following information was supplied regarding data availability:

The analysis of molecular dynamics simulations are available in the Supplemental Figures.

The input files and trajectories of molecular simulations of the three replicates of the KFDV vaccine construct are available at Figshare: Kasibhatla, Sunitha; Rajan, Lekshmi S.; Shete-Aich, Anita; Jani, Vinod; Patil, Savita; Joshi, Yash; et al. (2024). KFDV vaccine construct molecular simulations data. Figshare. Journal contribution. https://doi.org/10.6084/m9.figshare.26404432.v1.

## Supplemental Information

Supplemental information for this article can be found online at http://dx.doi.org/10.7717/peerj.18982#supplemental-information.

# REFERENCES

**Arumugam S, Varamballi P. 2021.** In-silico design of envelope-based multi-epitope vaccine candidate against Kyasanur forest disease virus. *Scientific Reports* **11**:17118 DOI 10.1038/s41598-021-94488-8.

**Barton GM. 2007.** Viral recognition by toll-like receptors. *Seminars in Immunology* **19(1)**:33–40 DOI 10.1016/j.smim.2007.01.003.

**Bhatia B, Meade-White K, Haddock E, Feldmann F, Marzi A, Feldmann H. 2021.** A live-attenuated viral vector vaccine protects mice against lethal challenge with Kyasanur Forest disease virus. *NPJ Vaccines* **6(1)**:152 DOI 10.1038/s41541-021-00416-2.

**Bhatia B, Tang-Huau TL, Feldmann F, Hanley PW, Rosenke R, Shaia C, Marzi A, Feldmann H. 2023.** Single-dose VSV-based vaccine protects against Kyasanur Forest disease in nonhuman primates. *Science Advances* **9(36)**:eadj1428 DOI 10.1126/sciadv.adj1428.

**Boittier ED, Tang YY, Buckley ME, Schuurs ZP, Richard DJ, Gandhi NS. 2020.** Assessing molecular docking tools to guide targeted drug discovery of CD38 inhibitors. *International Journal of Molecular Sciences* **21(15)**:5183 DOI 10.3390/ijms21155183.

**Boshell J, Rajagopalan PK. 1968.** Preliminary studies on experimental transmission of Kyasanur Forest disease virus by nymphs of Ixodes petauristae Warburton, 1933, infected as larvae on Suncus murinus and Rattus blanfordi. *Indian Journal of Medical Research* **56(4)**:589–593.

**Buchan DWA, Jones DT. 2019.** The PSIPRED protein analysis workbench: 20 years on. *Nucleic Acids Research* **47(W1)**:W402–W407 DOI 10.1093/nar/gkz297.

**Bui HH, Sidney J, Li W, Fusseder N, Sette A. 2007.** Development of an epitope conservancy analysis tool to facilitate the design of epitope-based diagnostics and vaccines. *BMC Bioinformatics* **8(1)**:361 DOI 10.1186/1471-2105-8-361.

**Case DA, Aktulga HM, Belfon K, Ben-Shalom IY, Brozell SR, Cerutti DS, Cheatham TE III, Cisneros GA, Cruzeiro VWD, Darden TA, Duke RE, Giambasu G, Gilson MK, Gohlke H, Goetz AW, Harris R, Izadi S, Izmailov SA, Jin C, Kasavajhala K, Kaymak MC, King E, Kovalenko A, Kurtzman T, Lee TS, LeGrand S, Li P, Lin C, Liu J, Luchko T, Luo R, Machado M, Man V, Manathunga M, Merz KM, Miao Y, Mikhailovskii O, Monard G, Nguyen H, O'Hearn KA, Onufriev A, Pan F, Pantano S, Qi R, Rahnamoun A, Roe DR, Roitberg A, Sagui C, Schott-Verdugo S, Shen J, Simmerling CL, Skrynnikov NR, Smith J, Swails J, Walker RC, Wang J, Wei H, Wolf RM, Wu X, Xue Y, York DM, Zhao S, Kollman PA. 2021.** Amber 2021. University of California, San Francisco. *Available at https://ambermd.org/doc12/Amber21.pdf*.

**Chen J, Ng MM, Chu JJ. 2015.** Activation of TLR2 and TLR6 by dengue NS1 Pprotein and its implications in the immunopathogenesis of dengue virus infection. *PLOS Pathogens* **11(7)**:e1005053 DOI 10.1371/journal.ppat.1005053.

**Chu JJ, Ng ML. 2004.** Infectious entry of West Nile virus occurs through a clathrin-mediated endocytic pathway. *Journal of Virology* **78(19)**:10543–10555 DOI 10.1128/JVI.78.19.10543-10555.2004.

**Collins KW, Copeland MM, Brysbaert G, Wodak SJ, Bonvin AMJJ, Kundrotas PJ, Vakser IA, Lensink MF. 2024.** CAPRI-Q: the CAPRI resource evaluating the quality of predicted structures of protein complexes. *Journal of Molecular Biology* **436(17)**:168540 DOI 10.1016/j.jmb.2024.168540.

**Cuevas CD, Ross SR. 2014.** Toll-like receptor 2-mediated innate immune responses against Junín virus in mice lead to antiviral adaptive immune responses during systemic infection and do not affect viral replication in the brain. *Journal of Virology* **88(14)**:7703–7714 DOI 10.1128/JVI.00050-14.

**Dandawate CN, Desai GB, Achar TR, Banerjee K. 1994.** Field evaluation of formalin inactivated Kyasanur Forest disease virus tissue culture vaccine in three districts of Karnataka state. *Indian Journal of Medical Research* **99**:152–158.

**Devadiga S, McElroy AK, Prabhu SG, Arunkumar G. 2020.** Dynamics of human B and T cell adaptive immune responses to Kyasanur forest disease virus infection. *Scientific Reports* **10(1)**:15306 DOI 10.1038/s41598-020-72205-1.

**De Vries SJ, van Dijk ADJ, Bonvin AMJJ. 2006.** WHISCY: what information does surface conservation yield? Application to data-driven docking. *Proteins: Structure, Function, and Bioinformatics* **63(3)**:479–489 DOI 10.1002/prot.20842.

**Dey S, Pratibha M, Singh Dagur H, Rajakumara E. 2023.** Characterization of host receptor interaction with envelope protein of Kyasanur forest disease virus and predicting suitable epitopes for vaccine candidate. *Journal of Biomolecular Structure and Dynamics* **42(8)**:4110–4120 DOI 10.1080/07391102.2023.2218924.

**Dhanda SK, Gupta S, Vir P, Raghava GP. 2013.** Prediction of IL4 inducing peptides. *Clinical and Developmental Immunology* **2013(1)**:263952 DOI 10.1155/2013/263952.

**Dhanda SK, Vir P, Raghava GP. 2013.** Designing of interferon-gamma inducing MHC class-II binders. *Biology Direct* **8(1)**:30 DOI 10.1186/1745-6150-8-30.

**Dimitrov I, Bangov I, Flower DR, Doytchinova I. 2014.** AllerTOP v.2—a server for in silico prediction of allergens. *Journal of Molecular Modeling* **20(6)**:2278 DOI 10.1007/s00894-014-2278-5.

**Dodd KA, Bird BH, Khristova ML, Albariño CG, Carroll SA, Comer JA, Erickson BR, Rollin PE, Nichol ST. 2011.** Ancient ancestry of KFDV and AHFV revealed by complete genome analyses of viruses isolated from ticks and mammalian hosts. *PLOS Neglected Tropical Diseases* **5(10)**:e1352 DOI 10.1371/journal.pntd.0001352.

**Dominguez C, Boelens R, Bonvin AMJJ. 2003.** HADDOCK: a protein–protein docking approach based on biochemical or biophysical information. *Journal of the American Chemical Society* **125(7)**:1731–1737 DOI 10.1021/ja026939x.

**Dowling W, Thompson E, Badger C, Mellquist JL, Garrison AR, Smith JM, Paragas J, Hogan RJ, Schmaljohn C. 2007.** Influences of glycosylation on antigenicity, immunogenicity, and protective efficacy of Ebola virus GP DNA vaccines. *Journal of Virology* **81(4)**:1821–1837 DOI 10.1128/JVI.02098-06.

**Doytchinova IA, Flower DR. 2007.** VaxiJen: a server for prediction of protective antigens, tumour antigens and subunit vaccines. *BMC Bioinformatics* **8(1)**:4 DOI 10.1186/1471-2105-8-4.

**Fumagalli MJ, Figueiredo LTM, Aquino VH. 2021.** Linear and continuous flavivirus epitopes from naturally infected humans. *Frontiers in Cellular and Infection Microbiology* **11**:710551 DOI 10.3389/fcimb.2021.710551.

**Funderburg N, Lederman MM, Feng Z, Drage MG, Jadlowsky J, Harding CV, Weinberg A, Sieg SF. 2007.** Human β-defensin-3 activates professional antigen-presenting cells via toll-like receptors 1 and 2. *Proceedings of the National Academy of Sciences* **104(47)**:18631–18635 DOI 10.1073/pnas.0702130104.

**Gasteiger E, Hoogland C, Gattiker A, Duvaud S, Wilkins MR, Appel RD, Bairoch A. 2005.** Protein identification and analysis tools on the Expasy server. In: Walker JM, ed. *The Proteomics Protocols Handbook*. Totowa: Humana Press, 571–607.

**Gladson V, Moosan H, Mathew S, Dineesh P. 2021.** Clinical and laboratory diagnostic features of Kyasanur Forest disease: a study from Wayanad, South India. *Cureus* **13(12)**:e20194 DOI 10.7759/cureus.20194.

**Gould EA, Solomon T. 2008.** Pathogenic flaviviruses. *Lancet* **371(9611)**:500–509 DOI 10.1016/S0140-6736(08)60238-X.

**Greenbaum J, Sidney J, Chung J, Brander C, Peters B, Sette A. 2011.** Functional classification of class II human leukocyte antigen (HLA) molecules reveals seven different supertypes and a surprising degree of repertoire sharing across supertypes. *Immunogenetics* **63(6)**:325–335 DOI 10.1007/s00251-011-0513-0.

**Gritsun DJ, Jones IM, Gould EA, Gritsun TS. 2014.** Molecular archaeology of Flaviviridae untranslated regions: duplicated RNA structures in the replication enhancer of flaviviruses and pestiviruses emerged via convergent evolution. *PLOS ONE* **9(3)**:e92056 DOI 10.1371/journal.pone.0092056.

**Gupta S, Kapoor P, Chaudhary K, Gautam A, Kumar R, Raghava GPS. 2015.** Peptide toxicity prediction. In: Zhou P, Huang J, eds. *Computational Peptidology*. New York, NY: Springer, 143–157 DOI 10.1007/978-1-4939-2285-7_7.

**Hafeez S, Achur R, Kiran SK, Thippeswamy NB. 2023.** Computational prediction of B and T-cell epitopes of Kyasanur forest disease virus marker proteins towards the development of precise diagnosis and potent subunit vaccine. *Journal of Biomolecular Structure and Dynamics* **41(18)**:9157–9176 DOI 10.1080/07391102.2022.2141882.

**Heinz FX, Stiasny K. 2012.** Flaviviruses and flavivirus vaccines. *Vaccine* **30(29)**:4301–4306 DOI 10.1016/j.vaccine.2011.09.114.

**Ikram A, Alzahrani B, Zaheer T, Sattar S, Rasheed S, Aurangzeb M, Ishaq Y. 2023.** An in silico deep learning approach to multi-epitope vaccine design: a Hepatitis E virus case study. *Vaccines* **11(3)**:710 DOI 10.3390/vaccines11030710.

**Ismail S, Ahmad S, Azam SS. 2020.** Immunoinformatics characterization of SARS-CoV-2 spike glycoprotein for prioritization of epitope-based multivalent peptide vaccine. *Journal of Molecular Liquids* **314**:113612 DOI 10.1016/j.molliq.2020.113612.

**Jespersen MC, Peters B, Nielsen M, Marcatili P. 2017.** BepiPred-2.0: improving sequence-based B-cell epitope prediction using conformational epitopes. *Nucleic Acids Research* **45(W1)**:W24–W29 DOI 10.1093/nar/gkx346.

**Kalyaanamoorthy S, Minh BQ, Wong TKF, Von Haeseler A, Jermiin LS. 2017.** ModelFinder: fast model selection for accurate phylogenetic estimates. *Nature Methods* **14(6)**:587–589 DOI 10.1038/nmeth.4285.

**Kasabi GS, Murhekar MV, Sandhya VK, Raghunandan R, Kiran SK, Channabasappa GH, Mehendale SM. 2013a.** Coverage and effectiveness of Kyasanur forest disease (KFD) vaccine in Karnataka, South India, 2005–2010. *PLOS Neglected Tropical Diseases* **7(1)**:e2025 DOI 10.1371/journal.pntd.0002025.

**Kasabi GS, Murhekar MV, Yadav PD, Raghunandan R, Kiran SK, Sandhya VK, Channabasappa GH, Mishra AC, Mourya DT, Mehendale SM. 2013b.** Kyasanur forest disease, India, 2011–2012. *Emerging Infectious Diseases* **19(2)**:278–281 DOI 10.3201/eid1902.120544.

**Katoh K, Rozewicki J, Yamada KD. 2019.** MAFFT online service: multiple sequence alignment, interactive sequence choice and visualization. *Briefings in Bioinformatics* **20(4)**:1160–1166 DOI 10.1093/bib/bbx108.

**Kim J, Yang YL, Jang SH, Jang YS. 2018.** Human β-defensin 2 plays a regulatory role in innate antiviral immunity and is capable of potentiating the induction of antigen-specific immunity. *Virology Journal* **15(1)**:124 DOI 10.1186/s12985-018-1035-2.

**Kiran SK, Pasi A, Kumar S, Kasabi GS, Gujjarappa P, Shrivastava A, Mehendale S, Chauhan LS, Laserson KF, Murhekar M. 2015.** Kyasanur forest disease outbreak and vaccination strategy, Shimoga district, India, 2013-2014. *Emerging Infectious Diseases* **21(1)**:146–149 DOI 10.3201/eid2101.141227.

**Kumar S, Stecher G, Li M, Knyaz C, Tamura K. 2018.** MEGA X: molecular evolutionary genetics analysis across computing platforms. *Molecular Biology and Evolution* **35(6)**:1547–1549 DOI 10.1093/molbev/msy096.

**Kuno G. 2007.** Host range specificity of flaviviruses: correlation with in vitro replication. *Journal of Medical Entomology* **44(1)**:93–101 DOI 10.1603/0022-2585(2007)44[93:hrsofc]2.0.co;2.

**Laskowski RA, MacArthur MW, Moss DS, Thornton JM. 1993.** PROCHECK—a program to check the stereochemical quality of protein structures. *Journal of Applied Crystallography* **26(2)**:283–291 DOI 10.1107/S0021889892009944.

**Laskowski RA, Swindells MB. 2011.** LigPlot+: multiple ligand-protein interaction diagrams for drug discovery. *Journal of Chemical Information and Modeling* **51(10)**:2778–2786 DOI 10.1021/ci200227u.

**Letunic I, Bork P. 2021.** Interactive tree of life (iTOL) v5: an online tool for phylogenetic tree display and annotation. *Nucleic Acids Research* **49(W1)**:W293–W296 DOI 10.1093/nar/gkab301.

**Liu G, Song L, Beasley DWC, Putnak R, Parent J, Misczak J, Li H, Reiserova L, Liu X, Tian H, Liu W, Labonte D, Duan L, Kim Y, Travalent L, Wigington D, Weaver B, Tussey L. 2015.**

Immunogenicity and efficacy of flagellin-envelope fusion dengue vaccines in mice and monkeys. *Clinical and Vaccine Immunology* **22(5)**:516–525 DOI 10.1128/CVI.00770-14.

**Maier JA, Martinez C, Kasavajhala K, Wickstrom L, Hauser KE, Simmerling C. 2015.** ff14SB: improving the accuracy of protein side chain and backbone parameters from ff99SB. *Journal of Chemical Theory and Computation* **11(8)**:3696–3713 DOI 10.1021/acs.jctc.5b00255.

**Martin DP, Murrell B, Golden M, Khoosal A, Muhire B. 2015.** RDP4: detection and analysis of recombination patterns in virus genomes. *Virus Evolution* **1(1)**:vev003 DOI 10.1093/ve/vev003.

**Masignani V, Pizza M, Moxon ER. 2019.** The development of a vaccine against Meningococcus B using reverse vaccinology. *Frontiers in Immunology* **10**:751 DOI 10.3389/fimmu.2019.00751.

**Mehla R, Kumar SRP, Yadav P, Barde PV, Yergolkar PN, Erickson BR, Carroll SA, Mishra AC, Nichol ST, Mourya DT. 2009.** Recent ancestry of Kyasanur forest disease virus. *Emerging Infectious Diseases* **15(9)**:1431–1437 DOI 10.3201/eid1509.080759.

**Minh BQ, Schmidt HA, Chernomor O, Schrempf D, Woodhams MD, Von Haeseler A, Lanfear R. 2020.** IQ-TREE 2: new models and efficient methods for phylogenetic inference in the genomic era. *Molecular Biology and Evolution* **37(5)**:1530–1534 DOI 10.1093/molbev/msaa015.

**Modhiran N, Watterson D, Blumenthal A, Baxter AG, Young PR, Stacey KJ. 2017.** Dengue virus NS1 protein activates immune cells via TLR4 but not TLR2 or TLR6. *Immunology & Cell Biology* **95(5)**:491–495 DOI 10.1038/icb.2017.5.

**Modis Y, Ogata S, Clements D, Harrison SC. 2004.** Structure of the dengue virus envelope protein after membrane fusion. *Nature* **427(6972)**:313–319 DOI 10.1038/nature02165.

**Mondotte JA, Lozach PY, Amara A, Gamarnik AV. 2007.** Essential role of dengue virus envelope protein N glycosylation at asparagine-67 during viral propagation. *Journal of Virology* **81(13)**:7136–7148 DOI 10.1128/JVI.00116-07.

**Mukhopadhyay S, Kuhn RJ, Rossmann MG. 2005.** A structural perspective of the flavivirus life cycle. *Nature Reviews Microbiology* **3(1)**:13–22 DOI 10.1038/nrmicro1067.

**Murawski MR, Bowen GN, Cerny AM, Anderson LJ, Haynes LM, Tripp RA, Kurt-Jones EA, Finberg RW. 2009.** Respiratory syncytial virus activates innate immunity through Toll-like receptor 2. *Journal of Virology* **83(3)**:1492–1500 DOI 10.1128/JVI.00671-08.

**Nagpal G, Usmani SS, Dhanda SK, Kaur H, Singh S, Sharma M, Raghava GP. 2017.** Computer-aided designing of immunosuppressive peptides based on IL-10 inducing potential. *Scientific Reports* **7(1)**:42851 DOI 10.1038/srep42851.

**National centre for disease control (NCDC). 2018.** CD Alert: Kyasanur Forest disease: a public health concern. *Available at https://niv.icmr.org.in/images/pdf/newsletter/KFD_guidelines.pdf*.

**Naz S, Aroosh A, Caner A, Şahar EA, Toz S, Ozbel Y, Abbasi SW. 2023.** Immunoinformatics approach to design a multi-epitope vaccine against cutaneous leishmaniasis. *Vaccines* **11(2)**:339 DOI 10.3390/vaccines11020339.

**Naz A, Shahid F, Butt TT, Awan FM, Ali A, Malik A. 2020.** Designing multi-epitope vaccines to combat emerging coronavirus disease 2019 (COVID-19) by employing immuno-informatics approach. *Frontiers in Immunology* **11**:1663 DOI 10.3389/fimmu.2020.01663.

**Patil DY, Yadav PD, Shete AM, Nuchina J, Meti R, Bhattad D, Someshwar S, Mourya DT. 2017.** Occupational exposure of cashew nut workers to Kyasanur Forest disease in Goa, India. *International Journal of Infectious Diseases* **61(6)**:67–69 DOI 10.1016/j.ijid.2017.06.004.

**Pettersen EF, Goddard TD, Huang CC, Couch GS, Greenblatt DM, Meng EC, Ferrin TE. 2004.** UCSF Chimera—a visualization system for exploratory research and analysis. *Journal of Computational Chemistry* **25(13)**:1605–1612 DOI 10.1002/jcc.20084.

**Piccini LE, Castilla V, Damonte EB. 2015.** Dengue-3 virus entry into Vero cells: role of clathrin-mediated endocytosis in the outcome of infection. *PLOS ONE* **10(10)**:e0140824 DOI 10.1371/journal.pone.0140824.

**Pizza M, Scarlato V, Masignani V, Giuliani MM, Aricò B, Comanducci M, Jennings GT, Baldi L, Bartolini E, Capecchi B, Galeotti CL, Luzzi E, Manetti R, Marchetti E, Mora M, Nuti S, Ratti G, Santini L, Savino S, Scarselli M, Storni E, Zuo P, Broeker M, Hundt E, Knapp B, Blair E, Mason T, Tettelin H, Hood DW, Jeffries AC, Saunders NJ, Granoff DM, Venter JC, Moxon ER, Grandi G, Rappuoli R. 2000.** Identification of vaccine candidates against serogroup B meningococcus by whole-genome sequencing. *Science* **287(5459)**:1816–1820 DOI 10.1126/science.287.5459.1816.

**Pokidysheva E, Zhang Y, Battisti AJ, Bator-Kelly CM, Chipman PR, Xiao C, Gregorio GG, Hendrickson WA, Kuhn RJ, Rossmann MG. 2006.** Cryo-EM reconstruction of dengue virus in complex with the carbohydrate recognition domain of DC-SIGN. *Cell* **124(3)**:485–493 DOI 10.1016/j.cell.2005.11.042.

**Poli G, Martinelli A, Tuccinardi T. 2016.** Reliability analysis and optimization of the consensus docking approach for the development of virtual screening studies. *Journal of Enzyme Inhibition and Medicinal Chemistry* **31(sup2)**:167–173 DOI 10.1080/14756366.2016.1193736.

**Ponomarenko J, Bui HH, Li W, Fusseder N, Bourne PE, Sette A, Peters B. 2008.** ElliPro: a new structure-based tool for the prediction of antibody epitopes. *BMC Bioinformatics* **9**:514 DOI 10.1186/1471-2105-9-514.

**Rambaut A, Lam TT, Max Carvalho L, Pybus OG. 2016.** Exploring the temporal structure of heterochronous sequences using TempEst (formerly Path-O-Gen). *Virus Evolution* **2(1)**:vew007 DOI 10.1093/ve/vew007.

**Rappuoli R. 2000.** Reverse vaccinology. *Current Opinion in Microbiology* **3(5)**:445–450 DOI 10.1016/S1369-5274(00)00119-3.

**Rappuoli R, Bottomley MJ, D'Oro U, Finco O, De Gregorio E. 2016.** Reverse vaccinology 2.0: human immunology instructs vaccine antigen design. *Journal of Experimental Medicine* **213(4)**:469–481 DOI 10.1084/jem.20151960.

**Reynisson B, Alvarez B, Paul S, Peters B, Nielsen M. 2020.** NetMHCpan-4.1 and NetMHCIIpan-4.0: improved predictions of MHC antigen presentation by concurrent motif deconvolution and integration of MS MHC eluted ligand data. *Nucleic Acids Research* **48(W1)**:W449–W454 DOI 10.1093/nar/gkaa379.

**Rothan HA, Kumar M. 2019.** Role of endoplasmic reticulum-associated proteins in flavivirus replication and assembly complexes. *Pathogens* **8(3)**:148 DOI 10.3390/pathogens8030148.

**Shil P, Yadav P, Patil A, Balasubramanian R, Mourya D. 2018.** Bioinformatics characterization of envelope glycoprotein from Kyasanur forest disease virus. *Indian Journal of Medical Research* **147(2)**:195–202 DOI 10.4103/ijmr.IJMR_1445_16.

**Singh A, Thakur M, Sharma LK, Chandra K. 2020.** Designing a multi-epitope peptide-based vaccine against SARS-CoV-2. *Scientific Reports* **10(1)**:16219 DOI 10.1038/s41598-020-73371-y.

**Sippl MJ. 1993.** Recognition of errors in three-dimensional structures of proteins. *Proteins: Structure, Function, and Bioinformatics* **17(3)**:355–362 DOI 10.1002/prot.340170404.

**Sirmarova J, Salat J, Palus M, Hönig V, Langhansova H, Holbrook MR, Ruzek D. 2018.** Kyasanur Forest disease virus infection activates human vascular endothelial cells and monocyte-derived dendritic cells. *Emerging Microbes & Infections* **7(1)**:175 DOI 10.1038/s41426-018-0177-z.

**Stiasny K, Koessl C, Heinz FX. 2003.** Involvement of lipids in different steps of the flavivirus fusion mechanism. *Journal of Virology* **77(14)**:7856–7862 DOI 10.1128/JVI.77.14.7856-7862.2003.

**Suchard MA, Lemey P, Baele G, Ayres DL, Drummond AJ, Rambaut A. 2018.** Bayesian phylogenetic and phylodynamic data integration using BEAST 1.10. *Virus Evolution* **4(1)**:vey016 DOI 10.1093/ve/vey016.

**Tandale BV, Balakrishnan A, Yadav PD, Marja N, Mourya DT. 2015.** New focus of Kyasanur Forest disease virus activity in a tribal area in Kerala, India, 2014. *Infectious Diseases of Poverty* **4**:13 DOI 10.1186/s40249-015-0044-2.

**Trapido H, Rajagopalan PK, Work TH, Varma MG. 1959.** Kyasanur Forest disease. VIII. Isolation of Kyasanur Forest disease virus from naturally infected ticks of the genus Haemaphysalis. *Indian Journal of Medical Research* **47(2)**:133–138.

**Van der Schaar HM, Rust MJ, Waarts BL, van der Ende-Metselaar H, Kuhn RJ, Wilschut J, Zhuang X, Smit JM. 2007.** Characterization of the early events in dengue virus cell entry by biochemical assays and single-virus tracking. *Journal of Virology* **81(21)**:12019–12028 DOI 10.1128/JVI.00300-07.

**van Zundert GCP, Rodrigues JPGLM, Trellet M, Schmitz C, Kastritis PL, Karaca E, Melquiond ASJ, van Dijk M, de Vries SJ, Bonvin AMJJ. 2016.** The HADDOCK2.2 web server: user-friendly integrative modeling of biomolecular complexes. *Journal of Molecular Biology* **428(4)**:720–725 DOI 10.1016/j.jmb.2015.09.014.

**Weiskopf D, Angelo MA, De Azeredo EL, Sidney J, Greenbaum JA, Fernando AN, Broadwater A, Kolla RV, De Silva AD, de Silva AM, Mattia KA, Doranz BJ, Grey HM, Shresta S, Peters B, Sette A. 2013.** Comprehensive analysis of dengue virus-specific responses supports an HLA-linked protective role for CD8 + T cells. *Proceedings of the National Academy of Sciences* **110(22)**:E2046–E2055 DOI 10.1073/pnas.1305227110.

**Work T. 1958.** Russian spring-summer virus in India: Kyasanur Forest disease. *Progress in Medical Virology* **1**:248–279.

**Xagorari A, Chlichlia K. 2008.** Toll-like receptors and viruses: induction of innate antiviral immune responses. *The Open Microbiology Journal* **2(1)**:49–59 DOI 10.2174/1874285800802010049.

**Yadav PD, Albariño CG, Nyayanit DA, Guerrero L, Jenks MH, Sarkale P, Nichol ST, Mourya DT. 2018.** Equine Encephalosis virus in India, 2008. *Emerging Infectious Diseases* **24(5)**:898–901 DOI 10.3201/eid2405.171844.

**Yadav PD, Patil S, Jadhav SM, Nyayanit DA, Kumar V, Jain S, Sampath J, Mourya DT, Cherian SS. 2020.** Phylogeography of Kyasanur forest disease virus in India (1957–2017) reveals evolution and spread in the Western Ghats region. *Scientific Reports* **10(1)**:1966 DOI 10.1038/s41598-020-58242-w.

**Yadav P, Sahay R, Mourya D. 2018.** Detection of Kyasanur forest disease in newer areas of Sindhudurg district of Maharashtra State. *Indian Journal of Medical Research* **148(4)**:453–455 DOI 10.4103/ijmr.IJMR_1292_17.

**Zähringer U, Lindner B, Inamura S, Heine H, Alexander C. 2008.** TLR2—promiscuous or specific? A critical re-evaluation of a receptor expressing apparent broad specificity. *Immunobiology* **213(3–4)**:205–224 DOI 10.1016/j.imbio.2008.02.005.

**Zhang W, Chipman PR, Corver J, Johnson PR, Zhang Y, Mukhopadhyay S, Baker TS, Strauss JH, Rossmann MG, Kuhn RJ. 2003.** Visualization of membrane protein domains by cryo-electron microscopy of dengue virus. *Nature Structural & Molecular Biology* **10(11)**:907–912 DOI 10.1038/nsb990.

**Zheng M, Karki R, Williams EP, Yang D, Fitzpatrick E, Vogel P, Jonsson CB, Kanneganti TD. 2021.** TLR2 senses the SARS-CoV-2 envelope protein to produce inflammatory cytokines. *Nature Immunology* **22(7)**:829–838 DOI 10.1038/s41590-021-00937-x.

**Zhou X, Zheng W, Li Y, Pearce R, Zhang C, Bell EW, Zhang G, Zhang Y. 2022.** I-TASSER-MTD: a deep-learning-based platform for multi-domain protein structure and function prediction. *Nature Protocols* **17(10)**:2326–2353 DOI 10.1038/s41596-022-00728-0.